Sorpt.Stud., 2(1), June 2026, 1-7

INDONESIAN SCHOLAR SOCIETY

Sorption Studies

Journal homepage: https://journal.solusiriset.com/index.php/ss
e-ISSN: 3123-5697

Research Article

Adsorption of Malachite Green using Coconut Shell–Graphite Oxide (CS-GiO): Kinetic and Isotherm Studies

Hazzha Azzahra[1], Sulthan Napoleon[1], Patricya Inggrid Wilhelmina Bolilanga[1], Rahmat Basuki[1]*, Gunaryo[1], Dea Dwi Ananda[1], Mayang Fauziah Putri Kuntjahjono[1], Robith Alzamzami[1], Nugroho Adi Sasongko[2,3,4], Akhmad Rifai[2], Nuha[2]

[1]*Department of Chemistry, The Republic of Indonesia Defense University, Kawasan IPSC Sentul, Bogor 16810, Indonesia*

[2]*Research Center for Sustainable Production System and Life Cycle Assessment, National Research and Innovation Agency (BRIN), Banten 15314, Indonesia*

[3]*Energy Security Graduate Program, The Republic of Indonesia Defense University Bogor, 16810, Indonesia*

[4]*Murdoch University, 90 South St, Murdoch Western Australia 6150, Australia*

https://doi.org/10.55749/ss.v2i1.160
Received: 8 Mar 2026; Revised: 20 May 2026; Accepted: 11 Jun 2026; Published online: 16 Jun 2026; Published regularly: 30 Jun 2026

Abstract— Malachite green (MG) is a toxic cationic dye commonly found in textile wastewater and poses serious environmental and health risks. In this study, coconut shell–derived graphene oxide (CS-GiO) was synthesized and evaluated as an adsorbent for the removal of MG from aqueous solutions. The material was prepared through carbonization of coconut shells followed by a modified Hummers method to oxidize coconut shell graphite (CS-Gi) into graphene oxide. Prior to oxidation, the carbonized material was purified using HF treatment. Structural characterization using FTIR confirmed the presence of oxygen-containing functional groups, indicating successful oxidation of CS-Gi into CS-GiO. Meanwhile, XRD analysis revealed the characteristic (002) diffraction plane and showed that CS-GiO exhibited lower crystallinity compared to CS-Gi due to the incorporation of oxygen functional groups that disrupted the original crystalline structure. Adsorption behavior was evaluated through isotherm and kinetic studies. The adsorption equilibrium was better described by the Langmuir isotherm model (R^2 = 0.9957) than the Freundlich model (R^2 = 0.9617), indicating monolayer adsorption on relatively homogeneous active sites. The maximum adsorption capacity (qm) was 35.95 mg g^{-1}, with a Langmuir constant (KL) of 37873.42 L mol^{-1} and a separation factor (RL = 0.000995), confirming that the adsorption process is highly favorable. Kinetic analysis revealed that the adsorption follows the pseudo-second-order (PSO) model (R^2 = 0.99818), with a rate constant (k_2) of 813.63 g mol^{-1} min^{-1} and an equilibrium adsorption capacity of 0.000349 mol g^{-1}, suggesting a relatively rapid adsorption process. The adsorption mechanism is likely dominated by chemisorption, involving interactions between oxygen-containing functional groups on the CS-GiO surface and cationic MG molecules through electrostatic attraction, coordination interactions, and possible electron transfer. These findings demonstrate that CS-GiO derived from coconut shells is a promising adsorbent for the efficient removal of malachite green from aqueous systems.

Keywords— *Adsorption isotherm; Adsorption kinetics; Dye wastewater; Graphite oxide; Malachite green*

1. INTRODUCTION

The rapid expansion of the textile industry in recent decades has been primarily driven by escalating global demand for apparel products, coupled with population growth and evolving consumer lifestyles. Textile manufacturing processes are intrinsically reliant on the extensive use of synthetic dyes to impart desired color properties and enhance the commercial value of textile materials [1]. Nevertheless, the large-scale utilization of these dyes results in the generation of dye-laden wastewater, which represents a major source of industrial effluents when inadequately treated. The discharge of dye-containing effluents into aquatic environments adversely affects water quality by increasing turbidity and chromaticity, thereby reducing light penetration and impairing the photosynthetic activity of primary producers. Consequently, dissolved oxygen levels decline, disrupting aquatic ecosystems and favoring the proliferation of anaerobic microorganisms. Moreover, many textile dyes are chemically stable, poorly biodegradable, and exhibit

***Corresponding author**.
Email address: rhmtbsq@gmail.com

toxic as well as carcinogenic properties, enabling their persistence and bioaccumulation in aquatic organisms, which poses long-term ecological and health risks [2].

One of the synthetic dyes widely used is Malachite Green, which belongs to the triphenylmethane dye group. This dye is extensively applied due to its high color intensity, strong affinity for textile fibers, good color stability, and relatively low production cost, making it both effective and economically advantageous in dyeing processes. However, *malachite green* possesses a complex and stable aromatic chemical structure, rendering it resistant to biological and chemical degradation that can cause serious adverse effects, including toxic and carcinogenic impacts on human health [3]. Furthermore, significant threats to ecosystem balance and environmental sustainability.

Various techniques have been developed to address dye-containing wastewater, such as advanced oxidation processes, coagulation–flocculation, biodegradation, membrane filtration, and adsorption [3]. Among these methods, adsorption has emerged as one of the most widely applied approaches due to its simple operational, low cost, and minimal generation of harmful by-products. Moreover, adsorption is particularly effective for removing chemically stable and poorly biodegradable dyes, even at low concentrations. One promising adsorbent material for this purpose is *graphite oxide*, a derivative of graphite.

Graphite oxide is a graphite derivative produced through the oxidation of graphite, resulting in the introduction of various oxygen-containing functional groups, such as hydroxyl, epoxy, and carboxyl groups, on the basal planes and edges of the layers [4]. *Graphite oxide* can be synthesized from various carbon sources, such as coconut shell, an abundant biomass waste with high potential as a precursor material. Coconut shell is characterized by a high carbon content, a stable aromatic structure, wide availability, and low cost, making it a promising and sustainable carbon source for *graphite oxide* synthesis. Several methods have been developed for the synthesis of *graphite oxide*, including the Brodie, Staudenmaier, and Hummers methods, among which the Hummers method is one of the most widely used. The Hummers method offers several advantages, such as a relatively short synthesis time, high oxidation efficiency, and simpler experimental procedure [5-6].

Graphite oxide has been widely reported to exhibit significant advantages over pristine graphite, particularly in its application as an adsorbent for wastewater treatment. Numerous studies have demonstrated that the presence of oxygen-containing functional groups on the surface of *graphite oxide* plays a crucial role in enhancing hydrophilicity, effective surface area, and the density of active adsorption sites. These characteristics enable multiple interaction mechanisms between *graphite oxide* and pollutant molecules, thereby resulting in a higher adsorption capacity. Several previous studies have reported the successful use of *graphite oxide* as an efficient adsorbent for the removal of various contaminants from aqueous media, including anionic dyes, heavy metal ions, and persistent organic compounds, with high removal efficiencies [7], [8]. However, most existing studies have focused on *graphite oxide* synthesized from commercial graphite, while the utilization of alternative biomass-derived carbon sources, particularly coconut shell, and comprehensive investigations into their adsorption performance toward *malachite green* remain relatively limited. Therefore, further research is required to evaluate the potential of coconut shell–derived *graphite oxide* as an effective, sustainable, and environmentally friendly adsorbent for dye wastewater treatment.

This study aims to (1) synthesize *graphite oxide* derived from coconut shell biomass waste using the Hummers method, and (2) evaluate the adsorption performance of the synthesized adsorbent through adsorption isotherm and kinetic studies toward *malachite green* dye. The adsorption isotherms were investigated by fitting equilibrium adsorption data obtained from varying initial concentrations of *malachite green* to the Langmuir and Freundlich isotherm models. Adsorption kinetics were analyzed by applying time-dependent adsorption data to the Lagergren (pseudo-first-order) and Ho (pseudo-second-order) kinetic models.

2. EXPERIMENTAL SECTION

2.1. Materials

All chemicals (hydrofluoric acid, HF 40% utilized for the removal of silica impurities; hydrochloric acid, HCl 37%; sulfuric acid, H_2SO_4 98%; sodium nitrate, $NaNO_3$; potassium permanganate, $KMnO_4$; hydrogen peroxide, H_2O_2 30%; and Malachite Green) were pro-analysis provided by Merck®, Germany, without further treatment. Coconut shells were obtained from a home-based industry, Mitraaren, Bandung, Indonesia.

2.2. Instrumentation

Fourier transform infrared (FTIR, (Shimadzu Prestige 21) was performed to identify the functional groups of the material. The crystal analysis was conducted by the X-ray diffractometer (XRD, BRUKER AXS D8 ADVANCE ECO). A single-beam UV–Visible spectrophotometer (GENESYS series, Thermo Scientific) was used to measure the concentration of the solution.

2.3. Synthesis of graphite oxide from coconut shell (CS-GiO)

Graphite oxide was synthesized using a modified Hummers method. Coconut shells were crushed into 2–5 mm particles and carbonized at 200 °C for 1 h to obtain a partially carbonized precursor, which was subsequently ground and sieved to 100 mesh. The sample was washed with 40% HF at 45 °C for 3 h (acid-to-sample ratio 3:1) to remove impurities, filtered, rinsed with distilled water until neutral pH, dried at 110 °C for 12 h, and sieved to 200 mesh.

For oxidation, 2 g of the prepared sample and 0.5 g of $NaNO_3$ were added to 50 mL of H_2SO_4 and stirred for 30 min in an ice bath at 5 °C. Then, 6 g of $KMnO_4$ was gradually added, and the mixture was stirred for 3 h while maintaining the temperature at ~20 °C. The reaction was continued at 50 °C for 1 h, followed by the gradual addition of 100 mL and 200 mL of deionized water with stirring for 1 h each. Subsequently, 10 mL of 30% H_2O_2 was added, and the mixture was stirred for 30 min. The suspension was washed with 20% HCl (80 mL) and deionized water until neutral pH. The resulting precipitate was dried at 110 °C for 12 h to obtain CS-GiO powder, which was characterized using FTIR and XRD.

2.4. Adsorption isotherms of malachite green on graphite oxide

For the adsorption isotherm study, 10 mg of CS-GiO was weighed and contacted with 20 mL of malachite green solutions with varying initial concentrations of 10, 20, 30, 40, 50, and 75 ppm for 180 min. After adsorption, the suspension was filtered to collect the filtrate. The residual concentration of malachite green in the solution was determined using a UV–Visible spectrophotometer. The obtained adsorption data were subsequently fitted to the Langmuir and Freundlich isotherm models.

2.5. Adsorption kinetics of malachite green on graphite oxide

For the adsorption kinetics study, 10 mg of CS-GiO was weighed and contacted with 20 mL of malachite green solution at an initial concentration of 20 mg/L for contact times of 5, 10, 20, 30, 40, 50, 60, 75, 90, and 120 min. After adsorption, the suspension was filtered to obtain the filtrate. The residual concentration of malachite green was determined using a UV–Visible spectrophotometer, and the adsorption kinetics data were subsequently fitted to the Lagergren pseudo-first-order and Ho pseudo-second-order kinetic models.

3. RESULT AND DISCUSSION

3.1. Stucture Analysis

Graphite oxide derived from coconut shells (CS-GiO) was synthesized using a modified Hummers method through several systematic stages. Coconut shells were crushed into particles of 2–5 mm to increase the surface area, thereby enhancing the efficiency of the carbonization process. Carbonization was carried out at 200 °C for 1 h to obtain high-carbon char. At this temperature, the initial thermal decomposition of major biomass components such as cellulose and hemicellulose occurred, resulting in the formation of solid carbonaceous material (char). To remove inorganic impurities such as silica and other mineral components, the sample was treated with 40% HF. HF plays a crucial role in dissolving silicate-based impurities through the formation of soluble fluorosilicate complexes [9].

The oxidation step was performed using a modified Hummers method, originally developed by William S. Hummers and Richard E. Offeman, with certain adjustments in reaction conditions. The low temperature was essential to control the exothermic nature of the reaction and to prevent excessive oxidation. In this system, H_2SO_4 acts as an intercalating agent, expanding the interlayer spacing of the carbon structure, while $NaNO_3$ facilitates the initial oxidation and generation of reactive species. $KMnO_4$ serves as a strong oxidizing agent, converting the sp^2 carbon framework into oxygen-functionalized carbon containing hydroxyl (–OH), epoxy (C–O–C), carbonyl (C=O), and carboxyl (–COOH) groups. The reaction was terminated by adding 30% H_2O_2, which reduces residual permanganate ions and manganese dioxide to soluble Mn^{2+} ions, typically indicated by a color change of the suspension to yellowish. The product was washed with 20% HCl to remove residual manganese species, followed by repeated washing with deionized water until neutral pH was reached to ensure complete removal of acidic residues.

The functional groups of the synthesized materials were confirmed by FTIR analysis, as presented in **Figure 1.** A comparison between the spectra of CS-Gi and CS-GiO was performed to identify changes in functional groups resulting from the oxidation process using the modified Hummers method. Both samples exhibit a broad absorption band in the range of 3620–3624 cm^{-1}, which is attributed to the O–H stretching vibration. In CS-GiO, the –OH band at 3620 cm^{-1} appears more pronounced than in CS-Gi, indicating an increased number of hydroxyl groups after oxidation. These –OH groups may originate from phenolic hydroxyls or hydrated carboxylic groups, suggesting an enhancement in the hydrophilic nature of the material following oxidation [10].

A significant difference is also observed in the carbonyl (C=O) region. In CS-Gi, a band appears at approximately 1695 cm^{-1}, whereas in CS-GiO, the band shifts and becomes more intense at around 1712 cm^{-1}. The shift toward a higher wavenumber indicates an increased content of carbonyl-containing groups, such

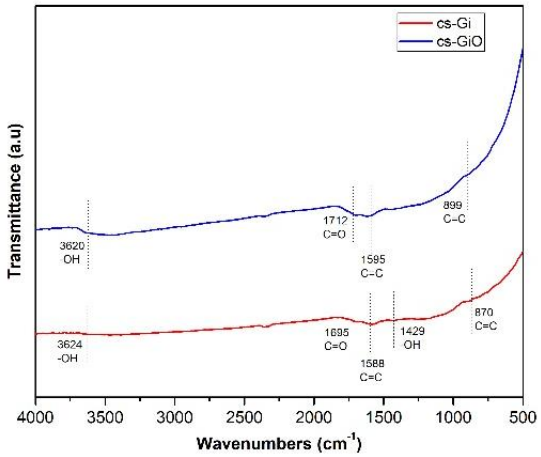

Figure 1. FTIR Spectrum of CS-GiO and CS-GiO

as ketones or carboxylic acids, formed during oxidation by $KMnO_4$. The more distinct C=O band in CS-GiO confirms that the sp² carbon framework has undergone oxidation, leading to the formation of new oxygen-containing functional groups. In the region of 1588–1595 cm^{-1}, bands corresponding to the aromatic C=C skeletal vibration of graphitic domains are observed. For CS-Gi, the band appears at 1588 cm^{-1}, while for CS-GiO it is detected at approximately 1595 cm^{-1}. Although the C=C band remains present in CS-GiO, its relative intensity decreases compared to the initial carbon material, indicating partial disruption of the sp² carbon network due to oxidation and the formation of functionalized sp³ carbon sites [11].

In the lower wavenumber region around 870–899 cm^{-1}, which is associated with out-of-plane aromatic C=C vibrations, a shift from 870 cm^{-1} (CS-Gi) to 899 cm^{-1} (CS-GiO) is observed. This shift indicates changes in the chemical environment of the aromatic rings due to the incorporation of oxygen-containing groups into the graphitic structure. Overall, the FTIR spectra demonstrate that the oxidation process effectively increases the abundance of oxygen-containing functional groups in the carbon material.

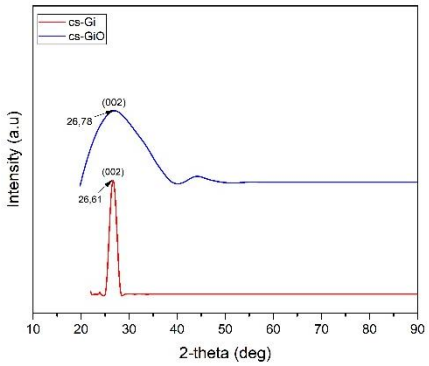

Figure 2. Diffractogram pattern cs Gi and cs GiO

The X-ray diffraction (XRD) pattern presented in **Figure 2** reveals a pronounced phase transformation from a crystalline structure to a more amorphous phase when graphite (Gi) is oxidized to GiO. This change is shown by the widening of the diffraction peak, which indicates a higher amount of amorphous phase in the material [9]. The material becomes even more amorphous when Gi is oxidized to GiO (**Figure 2**). Nevertheless, all samples exhibit relatively similar diffraction peaks in the range of 2θ ≈ 26.61° for Gi (d-spacing 2.91 Å) and 26.78° for GiO (d-spacing 3.75 Å). The peak within the 2θ range of 26.61–26.78° corresponds to the (002) crystallographic plane, which is characteristic of the graphite structure. The presence of this peak indicates that the synthesized materials still retain a certain degree of crystallinity.

Figure 2 reveals a pronounced structural transformation from a more crystalline graphite structure (Gi) to a more amorphous graphite oxide structure (GiO) after oxidation. This transformation is indicated by the significant broadening of the diffraction peak, suggesting decreased crystallinity, smaller ordered domains, and increased structural disorder due to the introduction of oxygen-containing functional groups [9,12]. The oxidation process disrupts the regular stacking of graphitic layers, resulting in a less ordered carbon structure. In addition, changes in the diffraction peak position indicate modifications in the interlayer spacing associated with the insertion of oxygen functional groups between the graphite layers. The reduced peak intensity and broader diffraction profile also suggest the possibility of partial exfoliation of the graphitic layers during oxidation. Nevertheless, both samples still exhibit diffraction peaks in the range of 2θ ≈ 26.61° for Gi and 26.78° for GiO, corresponding to the (002) crystallographic plane of graphite, indicating that a certain degree of graphitic structure is still retained after oxidation.

3.2. Adsorption Isotherms

The adsorption isotherm parameters are generated from the application of experimental data of concentration variations to the linear models of the Langmuir and Freundlich isotherms shown in **Equations (1)** and **(2)** [13].

$$\frac{C_e}{q_e} = \frac{1}{q_m K_L} + \frac{C_e}{q_m} \quad (1)$$

$$\log(q_e) = \log(K_F) + \frac{1}{n}\log(C_e) \quad (2)$$

The Langmuir model yielded a linear equation of y = 0.0278x + 0.268 with a coefficient of determination (R^2) of 0.9957, indicating an excellent fit of the adsorption data to this model (**Figure 3**). The high R^2 value suggests that the adsorption of malachite green (MG) onto CS-GiO follows the fundamental assumptions of the Langmuir isotherm, namely adsorption occurring on a homogeneous surface with identical active sites, the formation of a monolayer, and the absence of interactions between adsorbed molecules [13]. The

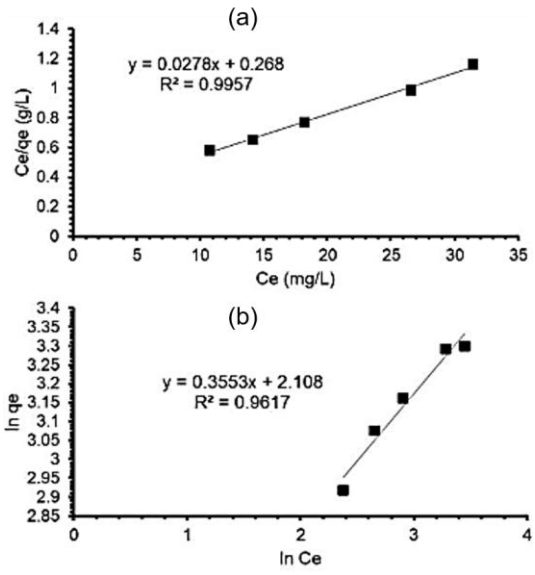

Figure 3. Adsorption malachite green by cs-GiO using (a) Langmuir and (b) Freundlich isotherm model

Langmuir parameters obtained include a maximum adsorption capacity (q_m) of 35.95 mg/g, a Langmuir constant (K_L) of 37873.42 L/mol, a separation factor (R_L) of 0.000995, and an R^2 of 0.9957. The q_m value indicates that CS-GiO possesses a relatively high adsorption capacity toward MG, while the R_L value, which lies between 0 and 1 and approaches zero, confirms that the adsorption process is highly favorable. Furthermore, the large KL value reflects a strong affinity between MG molecules and the CS-GiO surface. Overall, these findings confirm that the adsorption of MG onto CS-GiO proceeds predominantly through monolayer formation on a relatively homogeneous surface, consistent with the characteristics of the Langmuir isotherm model.

The Freundlich isotherm model produced a linear equation of y = 0.3553x + 2.108 with a coefficient of determination (R^2) of 0.9617. The corresponding parameters obtained were KF = 8.23 mg/g and n = 2.81, with R^2 = 0.9617. Although the R^2 value indicates a good correlation between the experimental data and the Freundlich model, it is lower than that of the Langmuir model (R^2 = 0.9957), suggesting that Freundlich can adequately describe the adsorption process, but not as well as Langmuir (**Table 1**). The value of n greater than 1 (n = 2.81) indicates that the adsorption process is favorable and likely dominated by physical adsorption (physisorption) with good adsorption intensity. Furthermore, the Freundlich model implies that the adsorbent surface is heterogeneous and allows for multilayer adsorption [14].

Comparatively, since the Langmuir model exhibits a higher R^2 value than the Freundlich model, the adsorption of malachite green onto CS-GiO is more appropriately described by the Langmuir isotherm. This suggests that the adsorption predominantly occurs as a monolayer on relatively homogeneous active sites. However, the reasonably high correlation with the Freundlich model also indicates that the CS-GiO surface is not entirely homogeneous, which is plausible considering that graphene oxide contains various oxygen-containing functional groups (–OH, –COOH, and epoxy groups) that create differences in adsorption energy. Overall, the adsorption of malachite green onto CS-GiO derived from coconut shell is highly favorable (RL < 1), exhibits a relatively high maximum adsorption capacity (35.95 mg/g), fits better with the Langmuir model indicating monolayer formation, and is supported by the Freundlich model with good adsorption intensity (n = 2.81). These findings demonstrate that CS-GiO has strong potential as an effective adsorbent for the removal of malachite green dye from aqueous solutions.

Table1. Langmuir and Freundlich parameters value

Isotherm models	Parameters	Value
Langmuir	b (mg/g)	35.95
	b ($\times 10^{-5}$ mol/g)	9.85
	K_L (L/mol)	37873.42
	E_L (kJ/mol)	26.12
	R^2	0.9957
Freundlich	B (mg/g)	8.23
	n	2.81
	R^2	0.9617

3.3. Adsortion Kinetics

Adsorption kinetics investigations were conducted using time-varying applications of the linear models of Lagergren **(Equation 3)** and Ho **(Equation 4)** [15-16]**.**

$$log q_e - q_t) = \log (q_e) - \frac{K_{Lag}}{2.303} t \quad (3)$$

$$\frac{t}{q_t} = \frac{1}{K_{Ho} {q_e}^2} + \frac{t}{q_e} \quad (4)$$

Based on the adsorption kinetic plot of the Lagergren or pseudo-first-order (PFO) model, the linear relationship between $\ln(q_e - q_t)$ and contact time (t) produced the regression equation y = −0.0434x − 8.9844 with a coefficient of determination (R^2) of 0.9850. The relatively high R^2 value indicates that the experimental data exhibit a good agreement with the pseudo-first-order kinetic model, suggesting that the adsorption process of malachite green (MG) onto CS-GiO can be reasonably described by this model. In the PFO model, the slope of the linear plot corresponds to $-k_1$, from which the adsorption rate constant (k_1) was calculated to be 0.0434 min^{-1}. This value reflects the adsorption rate of MG onto the surface of CS-GiO, where a higher k_1 value indicates a faster adsorption process. The intercept of −8.9844 corresponds to ln(qe), which represents the equilibrium adsorption capacity predicted by this kinetic model.

The relatively good fit of the data to the pseudo-first-order model suggests that the adsorption rate is influenced by the availability of active sites on the adsorbent surface and the concentration difference between the solute in the solution and that on the adsorbent surface. This model is generally associated with a physisorption mechanism, where the interactions involved are relatively weak, such as van der Waals forces or electrostatic interactions [17-20].

Based on kinetic modeling using the pseudo-second-order (PSO) model, the linear regression equation obtained was y = 2862.5x + 10071, with a coefficient of determination (R^2) of 0.99818. The very high R^2 value indicates that the PSO model exhibits an excellent fit to the experimental data for the adsorption of malachite green (MG) onto CS-GiO. From the calculation, the adsorption rate constant (k_2) was determined to be 813.63 g mol^{-1} min^{-1}, while the calculated equilibrium adsorption capacity (q_e,cal) was 0.000349 mol g^{-1}. In addition, the very small RMSE value of 3.96×10^{-6} and χ^2 value of 1.82×10^{-7} indicate that the deviation between the experimental data and the model prediction is minimal (**Table 2**). The calculated q_e value is also relatively close to the experimental value, further confirming that this model adequately represents the adsorption system.

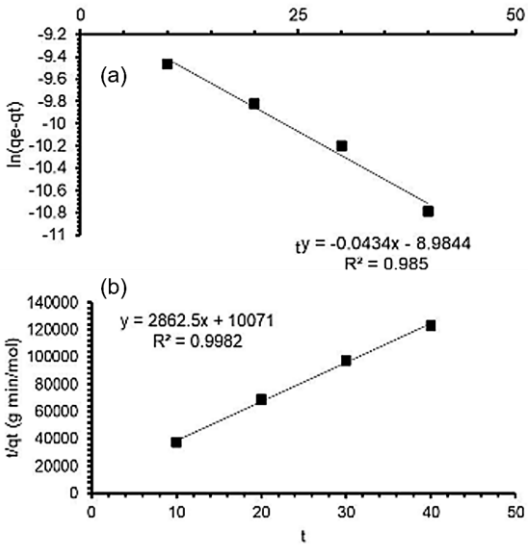

Figure 4. Malachite Green adsorption on CS-GiO as a function of time, and the linear model of the Lagergren (a) and Ho (b) adsorption kinetics models.

The relatively high k_{Ho} value suggests that the adsorption process occurs at a relatively fast rate. Mechanistically, the good agreement with the PSO model indicates that the adsorption process is likely governed by a chemisorption mechanism, involving chemical interactions between the active functional groups on the CS-GiO surface and malachite green molecules, such as electron exchange or the formation of chemical bonds [21-22].

Table 2. Kinetic parameters of Malachite Green adsorption on CS-GiO

Kinetics models	Parameters	Value
PFO	Calc. q_e (mol/g)	0.000125356
	K_{Lag} (min^{-1})	0.043369597
	RMSE q_e	0.000220028
	X^2	0.000560679
	R^2	0.9850
PSO	Calc. q_e (mol/g)	0.000349346
	K_{Ho} (g mol^{-1} min^{-1})	813.6327807
	RMSE q_e	0.00000396
	X^2	1.81789E-07
	R^2	0.9982

Note: q_e values in mg/g were calculated from mol/g based on the molecular weight of the adsorbate.

A comparison between the two kinetic models further reveals that the pseudo-second-order (PSO) model provides a better description of the adsorption process than the pseudo-first-order (PFO) model for malachite green adsorption onto CS-GiO. This is evidenced by the higher R^2 value obtained for the PSO model, as well as significantly lower error values (RMSE and χ^2) compared to those of the PFO model. Furthermore, the equilibrium adsorption capacity (q_e) predicted by the PSO model is more realistic and closer to the experimental value. Therefore, it can be concluded that the pseudo-second-order kinetic model is the most suitable model to describe the adsorption behavior of malachite green onto CS-GiO.

The suitability of this model suggests that the adsorption mechanism is predominantly controlled by chemisorption, which involves chemical interactions between the adsorbent and the adsorbate. These interactions may occur between the functional groups present on the GiO surface, such as –OH, –COOH, and other oxygen-containing groups, and the cationic groups of the malachite green molecule. Consequently, the adsorption process is not limited to weak physical interactions such as van der Waals forces, but may also involve electrostatic interactions, coordination bonding, and electron transfer mechanisms. This interpretation is consistent with the nature of malachite green as a cationic dye, which readily interacts with negatively charged surfaces or with active functional groups present on the adsorbent surface.

4. CONCLUSION

In this study, GiO from coconut shell was successfully synthesized and applied for the removal of Malachite Green from aqueous solution. Characterization results using FTIR and XRD confirmed the successful formation of the adsorbent and the presence of functional groups that potentially contribute to the adsorption process. The kinetic study demonstrated that the adsorption process follows the pseudo-second-order (PSO) model, as indicated by a higher coefficient of determination (R^2 = 0.9982) compared to the pseudo-first-order model (R^2 = 0.9850), along with significantly lower error values (RMSE = 3.96×10^{-6} and $\chi^2 = 1.82 \times 10^{-7}$). The calculated equilibrium adsorption capacity was 0.000349 mol g^{-1}, and the adsorption rate constant (k_2) was 813.63 g mol^{-1} min^{-1}, indicating a relatively rapid adsorption process. The good agreement with the PSO model suggests that the adsorption mechanism is predominantly controlled by chemisorption, involving chemical interactions between the functional groups present on the CS-GiO surface and the cationic malachite green molecules. These interactions may include electrostatic attraction, coordination interactions, and possible electron transfer mechanisms. Overall, the results indicate that CS-GiO exhibits promising potential as an effective adsorbent for the removal of malachite green from aqueous systems.

5. AUTHOR'S DECLARATION

5.1. Supporting Information

There is no supporting information in this paper. The data supporting this research's findings are available on request from the corresponding author (R.Basuki).

5.2. Acknowledgements

The authors sincerely acknowledge the financial support provided by the Department of Chemistry. Republic of Indonesia Defense University. The authors

also extend their gratitude for the facilities and laboratory resources made available by the BRIN.

5.3. Conflict of Interest

There was no conflict of interest in this study.

5.4. Author Contributions

HA & SN performed the conceptualization, investigation, methodology, writing original draft, review & editing. RB supervise the experiment, data calculations, and revise the manuscript. Gunaryo, NAS, AR, Nuha, DDA, MFPK, and RA collaborated on writing and revising the manuscript. All authors approved the final version of the manuscript.

5.5. AI Statement

Trinka AI was utilize to enhance the clarity, grammar, and overall readability of this manuscript. All technical content, data interpretation, and conclusion were solely developed and verified by the authors. The final version of the manuscript was thoroughly reviewed to ensure accuracy, coherence, and aligment with the study's findings.

6. REFERENCES

[1] Slama, H.B., Chenari Bouket, A., Pourhassan, Z., Alenezi, F.N., Silini, A., Cherif-Silini, H., Oszako, T., Luptakova, L., Golińska, P. and Belbahri, L. 2021. Diversity of synthetic dyes from textile industries, discharge impacts and treatment methods. *Appl. Sci.* 11(14). 6255. Doi: https://doi.org/10.3390/app11146255.

[2] Berradi, M., Hsissou, R., Khudhair, M., Assouag, M., Cherkaoui, O., El Bachiri, A. and El Harfi, A. 2019. Textile finishing dyes and their impact on aquatic environs. *Heliyon*. 5(11). e02711. doi: https://doi.org/10.1016/j.heliyon.2019.e02711.

[3] Bian, Y., Zhang, Y., Chen, Z.Y., Xu, L., Zhang, C.Y., Shi, D., Feng, X.S. and Wang, X.Q. 2025. Malachite green in environmental samples: Updates on sources, fates, distribution and removal techniques. *Ecotoxicol. Environ. Saf.* 303. 118978. doi: https://doi.org/10.1016/j.ecoenv.2025.118978.

[4] Shilyaeva, E.A. and Novakovskaya, Y.V. 2019. Functional groups of graphite oxide: experimental data and ab initio modeling. *Russ. J. Phys. Chem. A*. 93(10). 1908-1917. doi: https://doi.org/10.1134/S0036024419100273.

[5] Sujiono, E.H., Zabrian, D., Dahlan, M.Y., Amin, B.D. and Agus, J. 2020. Graphene oxide based coconut shell waste: synthesis by modified Hummers method and characterization. *Heliyon.* 6(8). e04568. doi: https://doi.org/10.1016/j.heliyon.2020.e04568.

[6] Asih, R., Yutomo, E.B., Ristiani, D., Baqiya, M.A., Kawamata, T., Kato, M., Watanabe, I., Koike, Y. and Darminto, D. 2019. Comparative study on magnetism of reduced graphene oxide (rGO) prepared from coconut shells and the commercial product. In *Mater. Sci. Forum.* 966. 290-295. doi: https://doi.org/10.4028/www.scientific.net/MSF.966.290.

[7] Mohammed, M.N., Aljibori, H.S.S., Jweeg, M.J., Al Oqaili, F., Abdullah, T.A., Abdullah, O.I., Meharban, F., Rashed, R.T., Aldulaimi, M. and Al-Azawi, K. 2024. A comprehensive review on graphene oxide based nanocomposites for wastewater treatment. *Polish J. Chem. Technol*. 26(1). 64-79. doi: https://doi.org/10.2478/pjct-2024-0007.

[8] Liu, X., Ma, R., Wang, X., Ma, Y., Yang, Y., Zhuang, L., Zhang, S., Jehan, R., Chen, J. and Wang, X. 2019. Graphene oxide-based materials for efficient removal of heavy metal ions from aqueous solution: A review. *Environ. Pollut.* 252. 62-73. doi: https://doi.org/10.1016/j.envpol.2019.05.050.

[9] Bolilanga, P.I.W., Basuki, R., Apriliyanto, Y.B., Prasojo, A.E., Lazuardy, A., Anitasari, R., Putri, R., Sasongko, N.A. and Santiko, A.B. 2024. Immobilization of Cerium(IV) Oxide onto reduced graphene oxide in epoxy resin matrix as radar absorbing composite for X-Band region. *Indones. J. Chem.,* 24(6). 1688-1700. doi: https://doi.org/10.22146/ijc.94404.

[10] Sharma, N., Sharma, V., Jain, Y., Kumari, M., Gupta, R., Sharma, S.K. and Sachdev, K. 2017. Synthesis and characterization of graphene oxide (GO) and reduced graphene oxide (rGO) for gas sensing application. *Macromol. Symp.* 376(1). 1700006. doi: https://doi.org/10.1002/masy.201700006.

[11] Kumar, H.V., Oyer, A.J., Huang, K.Y.S. and Adamson, D.H. 2022. Evolution of heterogeneity and chemical functionality during the oxidation of graphite. *Colloids and Interfaces.* 6(3). 44. doi: https://doi.org/10.3390/colloids6030044.

[12] Fahri, M., Bolilanga, P.I.W., Gunaryo, G., Stiawan, E. and Kurniadi, T., 2024. Exploring the potential of carbon-based radar absorbing material innovations. *Indones. J. Chem. Stud.* 3(2). 72-81. doi: https://doi.org/10.55749/ijcs.v3i2.56.

[13] Ngatijo, N., Gusmaini, N., Bemis, R. and Basuki, R. 2021. Adsorpsi methylene blue pada nanopartikel magnetit tersalut asam humat: kajian isoterm dan kinetika. *CHEESA Chem. Eng. Res. Artic.* 4(1). 51-64. doi: https://doi.org/10.25273/cheesa.v4i1.8433.51-64.

[14] Sah, M.K., Edbey, K., EL-Hashani, A., Almshety, S., Mauro, L., Alomar, T.S., AlMasoud, N. and Bhattarai, A. 2022. Exploring the biosorption of methylene blue dye onto agricultural products: A critical review. *Separations*. 9(9). 256. doi: https://doi.org/10.3390/separations9090256.

[15] Dehbi, A., Dehmani, Y., Omari, H., Lammini, A., Elazhari, K. and Abdallaoui, A. 2020. Hematite iron oxide nanoparticles (α-Fe2O3): synthesis and modelling adsorption of malachite green. *J. Environ. Chem. Eng.* 8(1). 103394. doi: https://doi.org/10.1016/j.jece.2019.103394.

[16] Basuki, R., Apriliyanto, Y.B., Stiawan, E., Pradipta, A.R., Rusdiarso, B. and Putra, B.R. 2025. Magnetic hybrid chitin-horse manure humic acid for optimized Cd (II) and Pb (II) adsorption from aquatic environment. *Case Stud. Chem. Environ. Eng.* 11. 101138. doi: https://doi.org/10.1016/j.cscee.2025.101138.

[17] Dive, A.M., Song, M.K. and Banerjee, S. 2017. Physisorption mechanism of solvated polysulfide chains on graphene oxides with varied functional groups. *J. Phys. Chem. C*. 121(9). 5089-5098. doi: https://doi.org/10.1021/acs.jpcc.6b12468.

[18] Kuntjahjono, M.F.P., Lestari, A.P., Nurhalimah, S., Sarweswara, W., Purba, F.O., Kaunang, A.M., Sasongko, N.A. and Basuki, R., 2025. Synthesis of Fe_3O_4 using the Co-precipitation method with temperature and time treatment as methylene blue adsorbent. *Sorpt. Stud.* 1(2). 48-53. doi: https://doi.org/10.55749/ss.v1i2.94.

[19] Aisyah, A.N., Sandri, A., Hutama, R.R., Kuntjahjono, M.F.P., Napoleon, S., Basuki, R. 2025. Synthesis of magnetite/chitin/fulvic acid derived from goat manure compost and adsorption study of Zn (II) for water security enhancement. *Sorpt. Stud.* 1(1). 34-41. doi: https://doi.org/10.55749/ss.v1i1.82.

[20] Ananda, D.D., Napoleon, S., Tarigan, T.O.J., Yulita, T.R., Alivia, L.S., Kusuma, B., Fajri, M.R., Putri, K.S., Artdero, N.V., Hartono, R., Basuki, R. 2025. Effect of different temperatures in magnetite synthesis on methylene blue adsorption. *Sorpt. Stud.* 1(2). 42-47. doi: https://doi.org/10.55749/ss.v1i2.84.

[21] Kavci, E., 2021. Malachite green adsorption onto modified pine cone: Isotherms, kinetics and thermodynamics mechanism. *Chem. Eng. Commun.* 208(3). 318-327. doi: https://doi.org/10.1080/00986445.2020.1715961.

[22] Hutama, R.R., Aisyah, A.N., Sandri, A., Kuntjahjono, M.F.P., Napoleon, S., Apriliyanto, Y.B., Sasongko, N.A., Basuki, R. 2025. Adsorption Ni(II) on magnetic fulvic acid-chitosan: kinetics and isotherm study. *Sorpt. Stud.* 1(1). 13-20. doi: https://doi.org/10.55749/ss.v1i1.79.